Pertanika J. Sci. & Technol. 32 (5): 2369 - 2384 (2024)

PERTANIKA JOURNALS

SCIENCE & TECHNOLOGY

Journal homepage: http://www.pertanika.upm.edu.my/

Finite Element Analysis of a Portable Bamboo Girder Used in Emergency Responses

Azrul Affandhi Musthaffa[1]*, Norazman Mohamad Nor[1], Abdulrahman Alhayek[2], Mohammed Alias Yusof[1] and Mohd Yuhazri Yaakob[3]

[1]Faculty of Engineering, Universiti Pertahanan Nasional Malaysia, Sungai Besi, Kuala Lumpur 57000, Malaysia
[2]Civil Engineering Department, College of Engineering, Universiti Tenaga Nasional, Jalan IKRAM - UNITEN, 43000 Kajang, Selangor, Malaysia
[3]Faculty of Engineering, Universiti Teknikal Malaysia Melaka (UTeM), Hang Tuah Jaya, 76100 Durian Tunggal, Melaka, Malaysia

ABSTRACT

This study uses numerical simulation to explore the performance of a portable bamboo girder designed for emergency scenarios and compares it to its steel counterpart. It underscores bamboo's appeal, offering a lightweight, quickly deployable, and eco-friendly alternative to steel. The research aims to assess bamboo's viability in emergency bridge construction, utilising SOLIDWORKS and ANSYS to create and simulate bamboo and steel girders. A bamboo girder aimed at humanitarian assistance and disaster relief (HADR) operations was analysed through ANSYS software under a Toyota Hilux truck's weight. Material properties, loads, and boundary conditions were defined for an accurate simulation. Three individual bamboo culms were tested in four-point flexural experiments, and the results revealed a modulus of elasticity of 14583 MPa and a local failure due to crushing and splitting with an ultimate strength of 263 MPa. Finite element analysis results indicated that the bamboo girder had a stress of 85.56 MPa and a deflection of 84.68 mm. Although the steel girder showed lower deflection, it had significantly higher stresses and weighed 180% more than the bamboo version. The bamboo girder's deflection surpassed the recommended limit under a fully loaded truck, indicating room for improvement. However, stress analysis revealed that the bamboo's structural integrity remained below its design strength. Conversely, the steel girder

ARTICLE INFO

Article history:
Received: 08 December 2023
Accepted: 06 February 2024
Published: 26 August 2024

DOI: https://doi.org/10.47836/pjst.32.5.24

E-mail addresses:
azrulaffandhi.aa@gmail.com (Azrul Affandhi Musthaffa)
azman@upnm.edu.my (Norazman Mohamad Nor)
rahman.hayek@gmail.com (Abdulrahman Alhayek)
alias@upnm.edu.my (Mohammed Alias Yusof)
yuhazri@utem.edu.my (Mohd Yuhazri Yaakob)
* Corresponding author

ISSN: 0128-7680
e-ISSN: 2231-8526

exhibited higher stresses and considerably greater weight. Despite deflection concerns, the bamboo girder demonstrated structural soundness and lower weight compared to steel. This positions it as a viable solution for swift emergency deployment, warranting further refinement for enhanced performance.

Keywords: Bamboo girder, finite element method, simulation, sustainability

INTRODUCTION

Sustainable development and green technology have become the major engineering themes in the 21st century, specifically in civil and structural engineering. New environmentally friendly materials such as composite polymer and bio-composite materials are developed to partially replace conventional construction materials such as steel and concrete (Rahman et al., 2023; Najeeb et al., 2023). On the other hand, bamboo has been identified as one of the alternative construction materials for building and bridge structures. Bamboo is abundant and well-known for its ability to withstand high bending stress, tensile stress and compressive stress, according to Bahari and Krause (Bahari & Krause, 2016). Apart from exhibiting a high strength-to-weight ratio, bamboo culms are fast-growing, mature in three years, and reach the peak of their strength. In China, bamboo was used to construct simple suspension bridges by splitting the bamboo to make cables or twisting whole culms of pliable bamboo together (Akinlabi et al., 2017; Liu et al., 2018). The utilisation of bamboo as an alternative construction material for buildings and bridges has been widely known. Modern studies have proven the use of bamboo in the construction of houses (Salzer et al., 2016), multistorey buildings (Yang et al., 2020) and various types of bridges (Amede et al., 2021). Because of its unique rhizome-dependent system, bamboo is one of the fastest-growing plants in the world, growing three times faster than most other plant species (Liu et al., 2022).

Additionally, bamboo can be utilised as a stand-alone material. Bamboo may be a viable substitute for steel, concrete, and masonry (Egoh et al., 2020; Auwalu & Dickson, 2019). Numerous bridges and expansive roofs with long spans have been erected in regions where bamboo cultivation thrives. An instance from 1937 involves the United States army, which ingeniously employed bamboo for a bridge in the Philippines (Chung & Yu, 2002). This bamboo bridge extended to 15 meters and showcased a remarkable capacity to endure a load of 16 kN. In contemporary times, bridge construction has leveraged laminated bamboo techniques. In 2006, the inaugural prototype of a bamboo bridge was introduced to experiment with laminated bamboo's application. Yan et al. (2010) documented the creation of girder samples composed of bamboo, subsequently utilised in erecting a 10-meter pedestrian bridge in Daozi. The bridge's surface was covered with precast concrete formed from reinforced bamboo strips. In addition, two

bamboo bridge projects in China have also shown that using nature-based solutions like bamboo can result in significantly fewer CO_2 emissions compared to similar bridges made of concrete or steel (Rong et al., 2022).

During peacetime, rapid bridging construction is needed to temporarily replace a damaged bridge caused by natural disasters such as floods, landslides, earthquakes or tsunamis. In this situation, a portable bridge is usually utilised while the new bridge is constructed. Portable bridging has been identified as the fastest and the most effective solution to open up the line of communication for Humanitarian Assistance and Disaster Relief (HADR) operations (Musthaffa et al., 2018). In this study, a portable bridge girder intended for small vehicles and made primarily from bamboo was modelled and analysed. The girder has some steel parts to hold the bamboo culms together, ensure they work as one unit, and provide a way to connect multiple segments as needed. The finite element numerical simulation was conducted using ANSYS software to investigate the girder's performance and deformation under the gross weight of a Toyota Hilux truck. This design provides a quick deployment time and the ability to expand for longer spans while being environmentally sustainable using a natural and lightweight material.

MATERIAL EXPERIMENT

Based on availability in Malaysia, Buluh Semantan (*Gigantochloa scortechinii*) bamboo harvested from Hulu Selangor was obtained at 3 to 5 years old. These bamboo culms have a length of around 4.58 m, an outer diameter between 95 and 120 mm with an average of 100 mm, and a thickness between 6 and 13 mm with an average of 10 mm.

In order to establish the properties of the bamboo members used in the analysis, a set of four-point bending experimental tests was conducted to assess the structural behaviour of the material under applied loads according to ISO 22157:2004 (ISO 22157-2:2004, 2004). The tests were conducted on three full bamboo tubes with a length of 4 m in a four-point bending setup, as shown in Figure 1. The setup consisted of a rigid steel frame with two fixed supports and two loading points spaced at a specific distance along the specimens according to the distance of nodes. ISO 22157:2004 defines the minimum free span of the culm to avoid failure by a transverse force to be 30D, where D is the outer diameter. This minimum span is around 3054 mm for the bamboo culms used in the experiments.

The specimens were positioned, and load was incrementally applied at a uniformly constant speed of 0.5 mm/s to induce bending. The test results revealed that the material failed locally due to crushing and splitting, as displayed in Figure 2. The average modulus of elasticity was 14583 MPa, and the average ultimate strength was 263 MPa, which will be used in the numerical simulation. The flexural test results are summarised in Table 1.

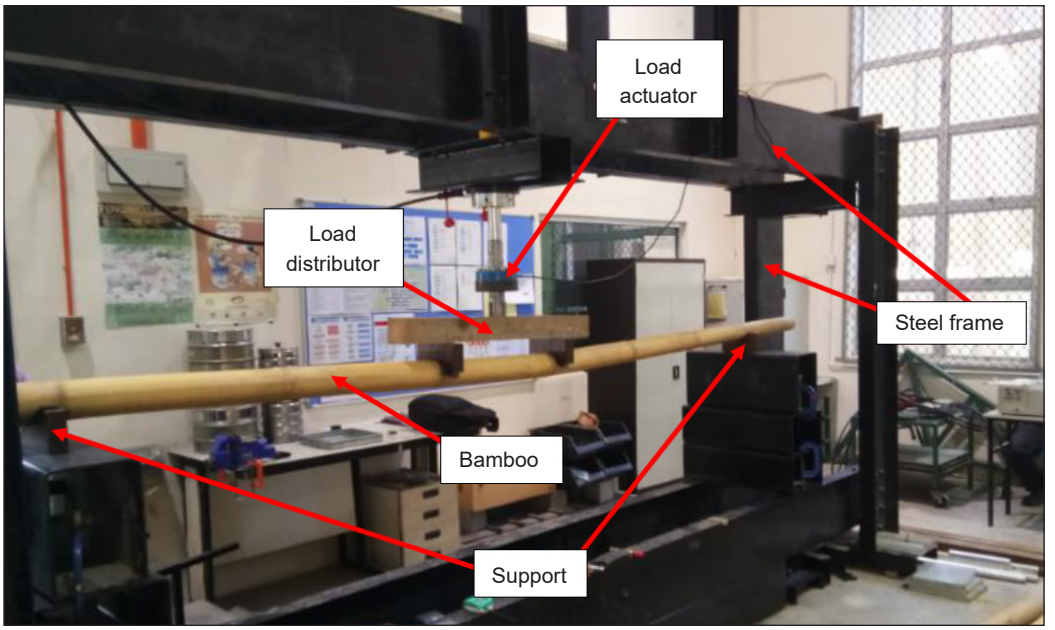

Figure 1. Test setup for bamboo in a four-point bending experiment

Figure 2. Local failure of bamboo due to crushing and splitting

Table 1
Summary of four-point bending experimental results

Sample ID	Inner diameter (mm)	Outer diameter (mm)	Thickness (mm)	Support span (mm)	Loading span (mm)	Modulus of elasticity (MPa)	Ultimate strength (MPa)
B1	80.5	98.3	8.9	3,260	580	13306.6	235.1
B2	78.3	104.5	13.1	3,760	855	15859.7	287.5
B3	78.8	102.4	11.8	3,450	765	14585.5	266.5
Average	79.2	101.8	11.3	-	-	14583.9	263.0

FINITE ELEMENT ANALYSIS METHODOLOGY

The 3D model of the girder is divided into two segments for ease of transportation and deployment. Each segment contains a 12-tube bamboo bundle, a steel connection at each end, and a steel plate on top. Figure 3 displays a flowchart for the methodology overview.

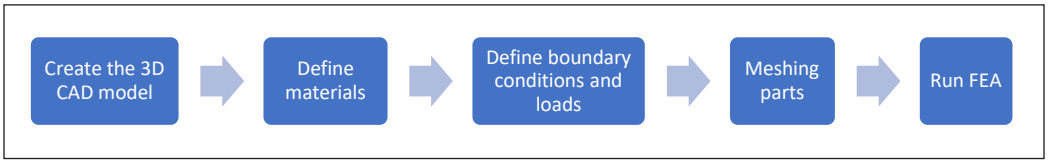

Figure 3. Methodology overview

Creating the 3D Model

The girder was created separately and assembled into the final girder in SOLIDWORKS. The bamboo bundle is 4 m long and is arranged in a 3×4 formation, as shown in Figure 4 (a). The average dimensions taken from Table 1 are used in creating the bamboo cross sections where each bamboo tube has an outer diameter of 100 mm and an inner diameter of 80 mm, giving the bundle a total width of 300 mm and a total depth of 400 mm. In addition, there are steel connections, which can be seen in Figure 4 (b), at each end with the same dimensions that provide a way to connect segments to create a longer-span girder. In order

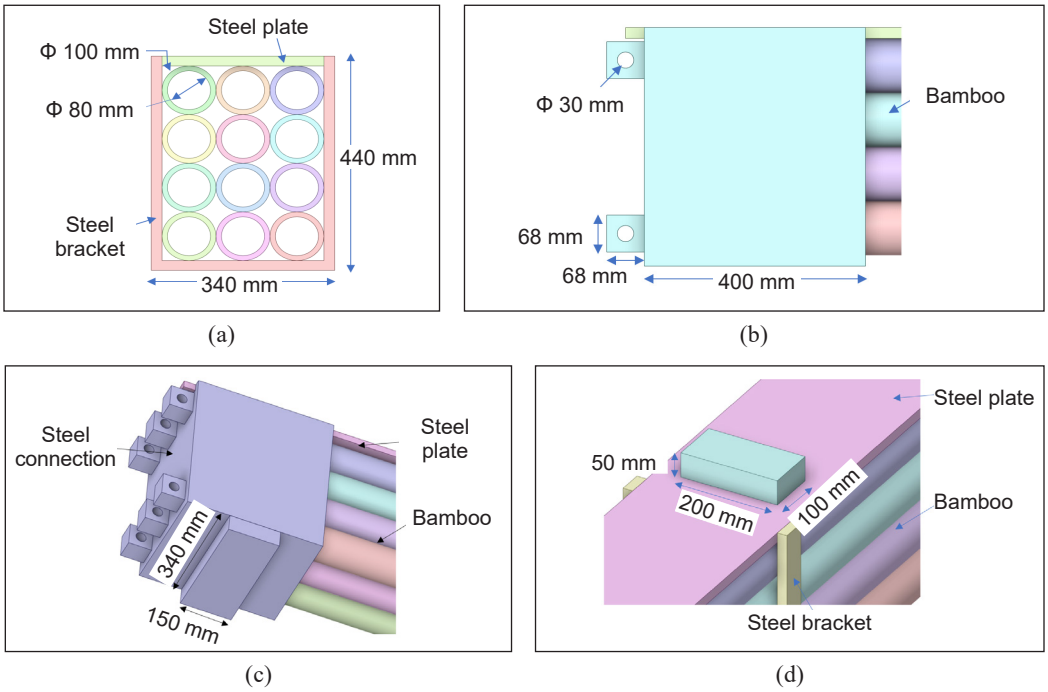

Figure 4. Parts dimensions: (a) cross-section of a bamboo bundle; (b) Steel connection; (c) Support pad; and (d) Loading pad

to keep the bundle in its 3×4 arrangement and work as one unit, four steel brackets were created at 800 mm spacing, as seen in Figure 5, each with a thickness of 20 mm. Moreover, load and support pads were created to apply the loading and boundary conditions on the girder, as displayed in Figures 4 (c) and (d). The loading pads' dimensions of 100×200 mm are the wheel patches that a car would form on the girder. At the same time, the loading span is 3085 mm based on the Toyota Hilux truck's dimensions and positioned on the girder to induce the maximum bending moment.

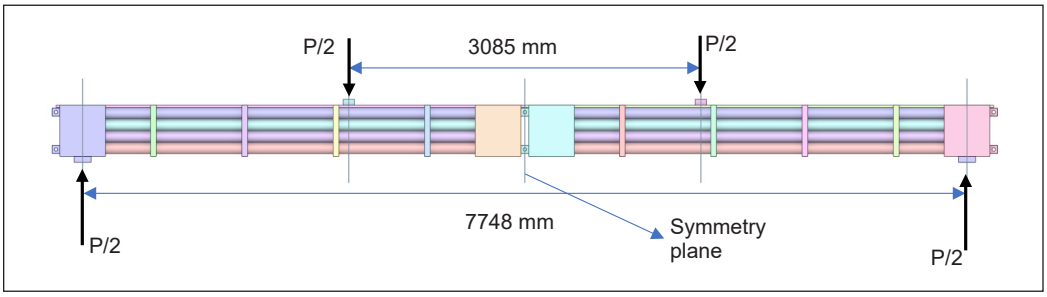

Figure 5. The full two segments girder

Generating the Numerical Model

After creating the fully assembled 3D model was transferred to ANSYS to generate the numerical model where materials are defined, loads and boundary conditions are assigned, and the simulation results are checked. Three materials were defined and used in the simulation, as shown in Table 2. A bamboo material is used for all the bamboo tubes, and structural steel is used for all the steel parts like the connections, brackets, and top plates. As for the loading and support pads, a soft, nearly incompressible material was created to transfer the loads while preventing stress concentrations at their locations and helping with convergence. The average modulus of elasticity obtained from the experimental flexural tests was used. On the other hand, design strength is used to assess the safety and feasibility of the bamboo girder design, which was obtained by utilising a factor of safety 1.5 for the ultimate strength, which would cover the uncertainty in bamboo strength, as shown in Equation 1.

$$Design\ strength = \frac{Ultimate\ strength}{1.5} \quad [1]$$

To take advantage of the symmetry in this girder and to reduce the computation time, only half of this girder was transferred to ANSYS, and a symmetry plane was created. As seen in Figure 5, the loading configuration follows the spacing and loads of a Toyota Hilux with a total gross weight of 28.5 kN. Furthermore, a dynamic amplification factor Φ that takes account of the dynamic magnification of stresses and vibration effects in the structure should be considered in a quasi-static analysis according to EN-1991-2 (Technical

Table 2
Material properties

Property	Bamboo	Structural Steel	Bearing Pads
Density (Kg/m³)	740	7850	1
Modulus of Elasticity (MPa)	14583	200000	70
Poisson's Ratio	0.3	0.3	0.4999
Ultimate Strength (MPa)	263	460	-
Design/Yield Strength (MPa)	175	250	-

Committee CEN, 2003). Although the code disregards the dynamic factor for vehicles moving at low speed (not more than 5 km/h), it requires the inclusion of a dynamic factor for vehicles moving at normal speed (70 km/h). For the case of a vehicle moving at normal speed, this factor is taken as illustrated in Equation 2:

$$\phi = 1.40 - \frac{L}{500} \geq 1 \quad [2]$$

where L is the span length for a simply supported girder in meters, it is around 1.3 for this girder, which makes the total load 37.05 kN. Since this girder is part of a bridge system consisting of 2 girders, only half of the total load was applied on this girder, which comes to P = 18.53 kN, giving each loading pad a downward force of 9.26 kN. Moreover, the self-weight of the girder was added by defining the standard earth gravity acceleration of 9.81 m/s², and fixed support was applied to the bottom of the support pads, as illustrated in Figures 6 and 7.

For meshing, ANSYS offers a comprehensive library of elements that covers a wide range of engineering problems such as thermal, fluid, stress and many more. In this simulation, higher-order 3D solid elements exhibiting quadratic displacement behaviour were used for accuracy. Most solid elements were SOLID186, a higher-order 3D 20-node solid element that exhibits quadratic displacement behaviour. This element is defined by 20 nodes with three degrees of freedom per node: translations in the directions of the nodal x, y, and z. In addition, some elements of SOLID187 were used, such as a higher order 3D, 10-node element with a quadratic displacement behaviour well suited to modelling irregular meshes. Both elements above can be seen in Figure 8.

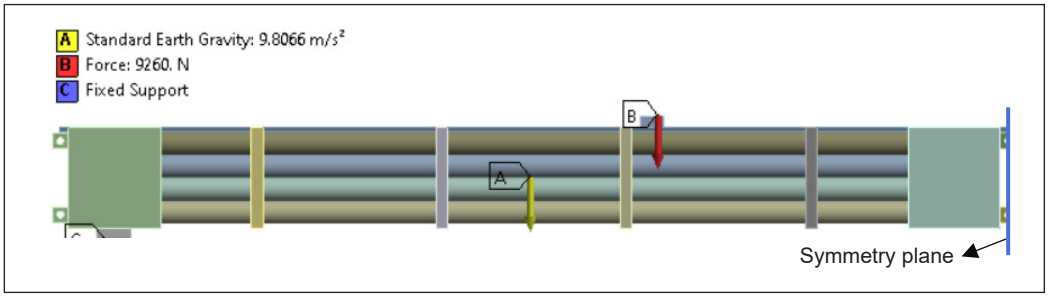

Figure 6. Defining self-weight, applied force, fixed support, and the symmetry plane

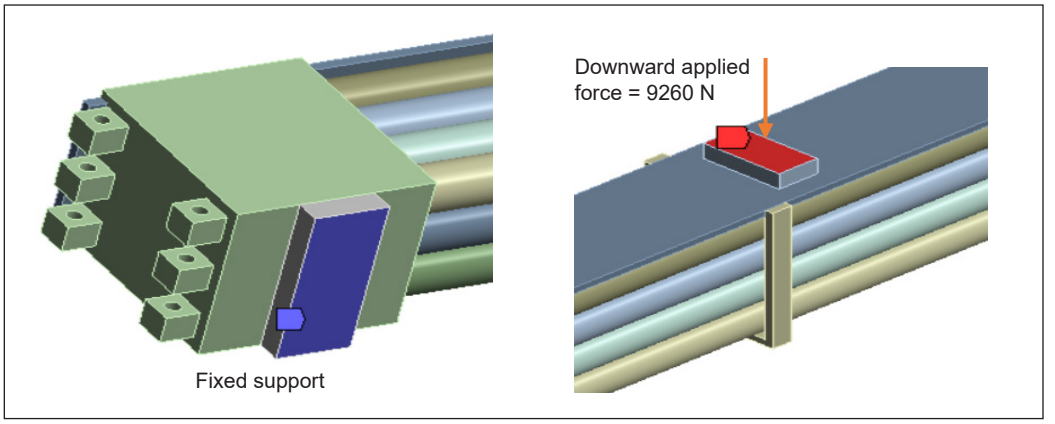

Figure 7. Defining boundary conditions and loads

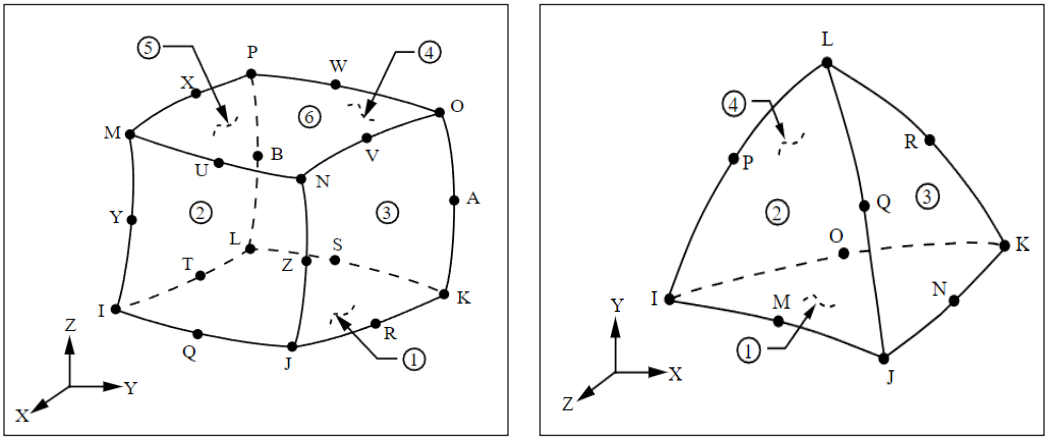

(a) (b)

Figure 8. The geometry, node locations, and the element coordinate system for: (a) SOLID186; and (b) SOLID187 (Ansys Inc., 2017)

Furthermore, a mesh independence check was conducted, starting with a 20 mm mesh size while checking the maximum equivalent stress in bamboo (Table 3). Increasing the number of elements over six times to nearly 525000 resulted in a slight decrease in the stress.

Therefore, a global size of 20 mm was chosen to balance accuracy with computational time, as seen in Figure 9. It resulted in a total number of nodes 270572 and a total number of solid elements 79803. ANSYS offers many types of contacts to define the behaviour between different parts coming into contact with each other, such as bonded, frictional, and frictionless. The contacts between the support and loading pads and the steel parts they touch were defined as bonded, a linear contact that prevents sliding and separation. The contacts and interactions between bamboo tubes were defined as frictional contact with a friction coefficient of 0.1, a nonlinear contact type that allows separation and sliding with some

Table 3
Mesh independence study

Iteration	Equivalent Stress Bamboo (MPa)	Change (%)	Nodes	Elements
1	85.564	-	270572	79803
2	83.977	-1.85	926570	526237

friction. Moreover, the contact between bamboo tubes and surrounding steel parts was also defined as frictional contact with a friction coefficient of 0.1. Accordingly, the total number of contact elements is found to be 64090. The contact pair elements used are CONTA174 and TARGE170. The first element, CONTA174, represents contact and sliding between 3D target surfaces and a deformable surface defined by this element. It has the same geometric characteristics as the solid or shell element face with which it is connected, and the contact occurs when the element surface penetrates an associated target surface. On the other hand, TARGE170 is used to represent various 3D "target" surfaces for the associated contact elements, such as CONTA174, where the contact elements themselves overlay the solid, shell, or line elements describing the boundary of a deformable body and are potentially in contact with the target surface. As for the steel parts, they are considered to be welded together, and as a result, a mesh continuity was provided between them.

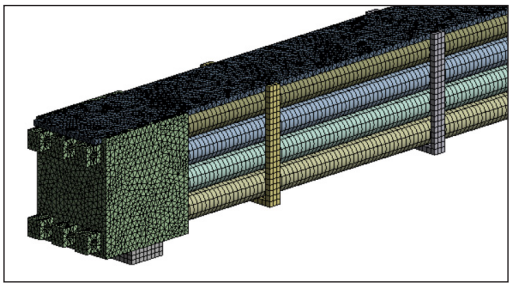

Figure 9. The meshing size is 20 mm

The Governing Equations

For many structures, it is difficult to determine the distribution of deformation and stress using conventional methods, and thus the finite element method (FEM) is necessarily used. This method is a powerful numerical technique for solving partial differential equations and analysing complex physical systems in engineering and science. FEM starts by creating what is known as a mesh which divides a complex physical domain into small elements connected at rigid points called nodes. Each element has a mathematical function, known as the shape function, which describes and approximates the behaviour of the physical quantities within the element based on the element's geometry and connectivity. Additionally, these elements are bound and behave according to the governing equations, which are the equations that define the principles of physics and describe the behaviour of the system under consideration. In the case of static structural analysis, they are (1) material constitutive equations, (2) equilibrium equations, and (3) displacement-strain equations. These equations express the relationships between the physical quantities and external forces, ensuring that equilibrium and other physical laws are satisfied.

Three primary methods can be used to derive the finite element equations of a physical system. These are (1) the direct method or direct equilibrium method for structural analysis problems, which is typically used in analytical hand calculations; (2) the variational methods, such as the principle of minimum of potential energy and the principle of virtual work, and (3) the weighted residual methods. While the direct method gives exact solutions, solving complicated cases is much more difficult. Therefore, finite element analysis programs use weak forms, such as the variational method, to describe the problem in integral form and give an approximate numerical solution.

ANSYS uses the principle of virtual work to derive the governing equations, which state, "If a deformable body in equilibrium is subjected to arbitrary virtual (imaginary) displacements associated with a compatible deformation of the body, the virtual work of external forces on the body is equal to the virtual strain energy of the internal stresses." The advantage of this principle over the minimum potential energy is that it applies more generally to both materials that behave in a linear elastic, as well as those that behave in a nonlinear fashion. Applying the principle to a finite element gives Equation 3:

$$\delta U^{(e)} = \delta W^{(e)} \quad [3]$$

Where $\delta U^{(e)}$ is the virtual strain energy due to internal stresses (the internal virtual work), and $\delta W^{(e)}$ is the virtual work of external forces on the element (the external virtual work). Another set of equations that relate stresses to strains are called the constitutive equations, which define the relationship between stress and strain within a material as in Equation 4:

$$\sigma_{ij} = C_{ijkl}\ \varepsilon_{kl} \quad [4]$$

where σ_{ij} is the stress components, C_{ijkl} is the components of the elastic stiffness tensor, and ε_{kl} is the strain components. These equations form the basis for solving three-dimensional stress analysis problems, where the goal is to determine the stress and strain distribution within a solid body subject to applied loads and boundary conditions. The specific form of these equations can be modified for different material behaviours and boundary conditions. For isotropic linear elastic materials, the relationship is as in Equation 5:

$$\begin{bmatrix} \sigma_1 \\ \sigma_2 \\ \sigma_3 \\ \tau_{23} \\ \tau_{13} \\ \tau_{12} \end{bmatrix} = \frac{E}{(1+\upsilon)(1-2\upsilon)} \begin{bmatrix} 1-\upsilon & \upsilon & \upsilon & 0 & 0 & 0 \\ \upsilon & 1-\upsilon & \upsilon & 0 & 0 & 0 \\ \upsilon & \upsilon & 1-\upsilon & 0 & 0 & 0 \\ 0 & 0 & 0 & \frac{(1-2\upsilon)}{2} & 0 & 0 \\ 0 & 0 & 0 & 0 & \frac{(1-2\upsilon)}{2} & 0 \\ 0 & 0 & 0 & 0 & 0 & \frac{(1-2\upsilon)}{2} \end{bmatrix} \begin{bmatrix} \varepsilon_1 \\ \varepsilon_2 \\ \varepsilon_3 \\ \gamma_{23} \\ \gamma_{13} \\ \gamma_{12} \end{bmatrix} \quad [5]$$

where E is the Young's modulus, and ν is Poisson's ratio. All aforementioned governing equations must satisfy the equilibrium equations, which. in the case of a 3D static stress state, are given by Equations 6, 7 and 8:

$$\frac{\partial \sigma_x}{\partial x} + \frac{\partial \tau_{xy}}{\partial y} + \frac{\partial \tau_{xz}}{\partial z} + \rho g_x = 0 \quad [6]$$

$$\frac{\partial \tau_{yx}}{\partial x} + \frac{\partial \sigma_y}{\partial y} + \frac{\partial \tau_{yz}}{\partial z} + \rho g_y = 0 \quad [7]$$

$$\frac{\partial \tau_{zx}}{\partial x} + \frac{\partial \tau_{zy}}{\partial y} + \frac{\partial \sigma_z}{\partial z} + \rho g_z = 0 \quad [8]$$

where σ is the normal stress, τ is the shear stress, $\tau_{xy} = \tau_{yx}$, $\tau_{xz} = \tau_{zx}$, and $\tau_{yz} = \tau_{zy}$, and ρg represents the body forces in three directions. Figure 10 shows the stress state of a 3D differential element in space.

The third governing equation for 3D static structural analysis is displacement-strain relations. It can be expressed in a matrix form by considering a vector of displacements (d) and a vector of strains (ε); the relationship is given by Equation 9:

$$\{\varepsilon\} = [B]\{d\} \quad [9]$$

where B is the strain-displacement matrix and d is the nodal displacement in each degree of freedom. Consequently, the element stiffness matrix is calculated by Equation 10:

$$[k] = \iiint [B]^T [C][B] dV \quad [10]$$

where B is the strain-displacement matrix, and C is the constitutive matrix. Assembling the element's stiffness matrix [k] into a global stiffness matrix [K] and the global nodal forces {F}, the nodal displacements {d} can be found from the global simple Equation 11:

$$\{F\} = [K]\{d\} \quad [11]$$

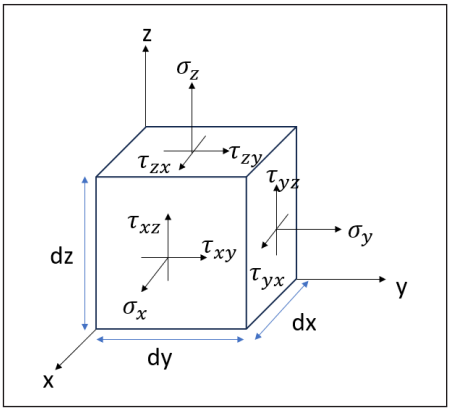

Figure 10. 3D stress state in a differential element

RESULTS AND DISCUSSION

A static structural analysis was carried out in ANSYS to evaluate the design of a bamboo girder used as a part of an emergency bridge system. Figure 11 shows the deformation of the girder along the Y-axis, which has a maximum downward deflection of 84.68 mm. In the American Association of State Highway and Transportation Officials (AASHTO) design guidelines 2020, deflection limitations are stated to be generally optional, except

for some cases, and some limits are given for steel, aluminium, and concrete vehicular bridges in the range of span/1000 to span/300, depending on the case. Since this girder is intended to be used as a temporary emergency system under small vehicles, the deflection limit is taken as span/100, which makes the limit for this girder 7748/100 = 77.48 mm. It indicates that a fully loaded pickup truck, similar to a Toyota Hilux, might be too heavy for the serviceability requirements of this girder.

The von-Mises stress for the bamboo tubes shows a maximum of 85 MPa, as shown in Figure 12 (a), much lower than the design strength of 175 MPa. Moreover, this maximum stress is concentrated at the nodes of the bottom three tubes, and more specifically, where the bamboos coincide with the edge of the steel connection at the support side, as seen in Figure 13 (a). Table 4 shows the utilisation ratio and demand over the capacity ratio of the bamboo tubes based on design strength.

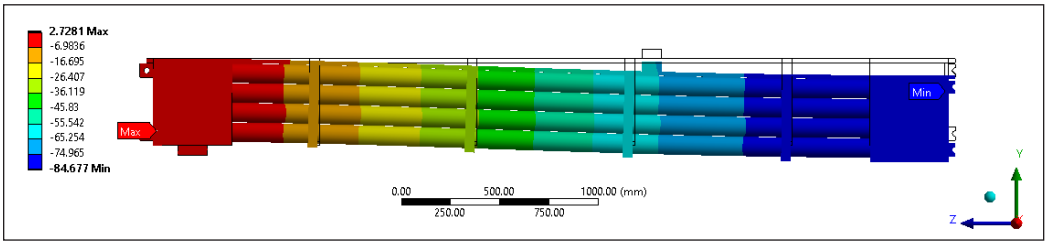

Figure 11. Directional deformation in the Y axis (true scale)

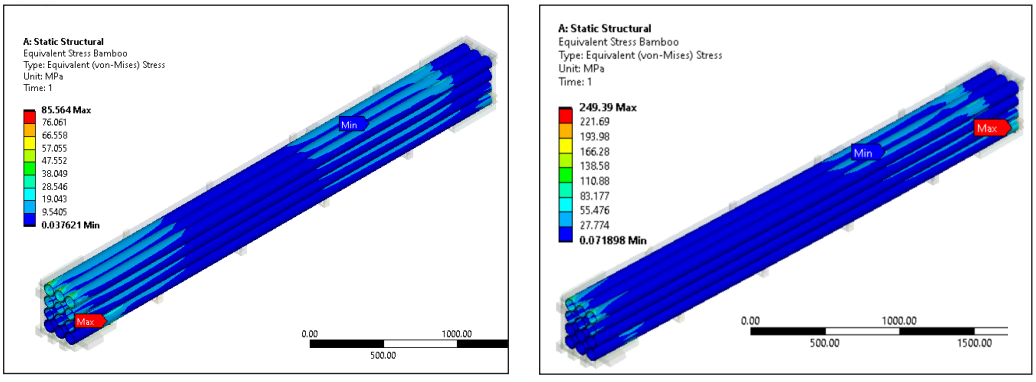

(a) (b)

Figure 12. Equivalent von-Mises stress: (a) bamboo tubes; and (b) steel tubes

Table 4
The utilisation ratio for the bamboo tubes based on design strength

	Bamboo tubes	**Utilisation (Design strength)**
Max Equivalent stress Bamboo (MPa)	85.564	0.49
Min Normal Stress-Z Bamboo (MPa)	102.53	0.59
Max Normal Stress-Z Bamboo (MPa)	42.342	0.24

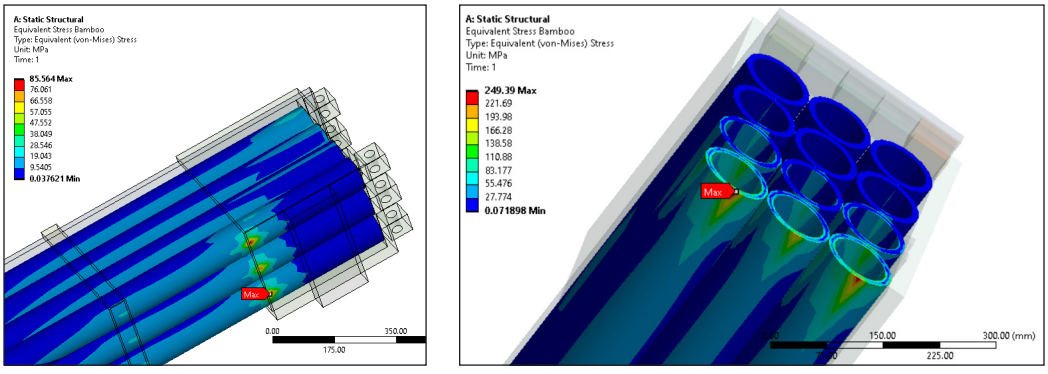

(a) (b)

Figure 13. The Equivalent von-Mises stress at the location of stress concentration: (a) bamboo tubes; and (b) steel tubes

Figure 14 shows the normal stress in the Z direction with a maximum compressive stress of 102.5 MPa and a maximum tensile stress of 42.3 MPa, much lower than the design stress of 175 MPa. The maximum compressive stress happens at the same location as the maximum von-Mises stress.

The von-Mises stress for the steel parts shows a maximum of 410 MPa, as shown in Figure 15, which is much higher than the yield strength of 250 MPa but lower than the ultimate strength of 460 MPa. This high stress could be explained, considering it was achieved at a single node, indicating a numerical singularity. In addition, this maximum stress is concentrated at the node connecting the top steel plate with a steel connection, as seen in Figure 16.

An identical girder was simulated using steel tubes to compare the performance of the bamboo girder. The results are summarised in Table 5, where the deformation was 70% lower using steel tubes, as expected due to their remarkably higher stiffness. However, the maximum equivalent stress in

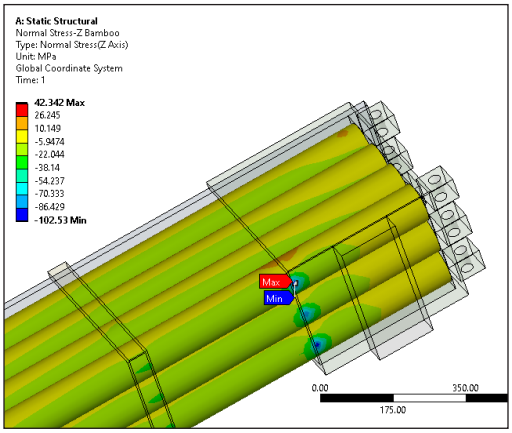

Figure 14. The location of the stress concentration on the bamboo tubes (normal stress Z axis)

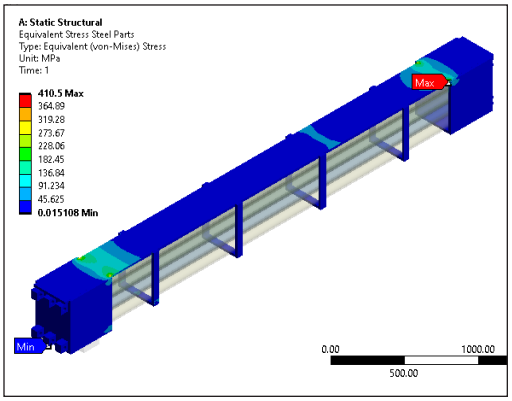

Figure 15. Equivalent von-Mises stress for the steel parts

the steel tubes was significantly higher, reaching the yield strength of 250 MPa, while the bamboo tubes stayed well below their design strength of 175 MPa, as shown in Figure 12. Nevertheless, the stress concentration was higher in the steel tubes, reaching 249.39 MPa at the middle span, Figure 13 (b), unlike the bamboo tubes, where the stress was much lower and concentrated at the support side, as seen in Figure 13 (a). Moreover, the total mass of the steel girder is almost 2.8 times the mass of the bamboo bridge, which makes it notably more difficult to carry and transport. Given that the main objective of this design is to be deployed quickly during emergencies, the relatively low weight of the bamboo girder gives it an advantage over its steel counterpart.

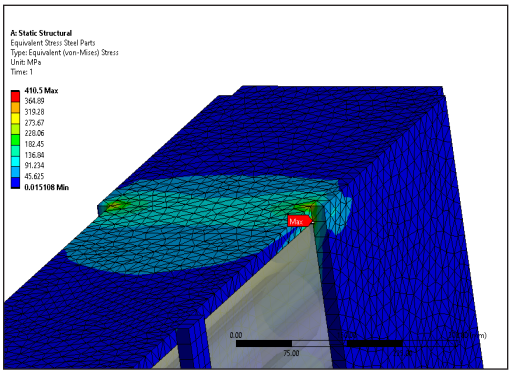

Figure 16. The location of the stress concentration on the steel parts (Equivalent von-Mises stress)

Table 5
Results comparison between bamboo tubes and steel tubes

2 Segments 4-point bending	Bamboo Tubes	Steel Tubes	Difference %
Load (N)	-9260	-9260	0%
Max deformation (mm)	84.678	25.53	70%
Max Equivalent stress tubes (MPa)	85.564	249.4	-191%
Min Normal Stress-Z tubes (MPa)	-102.53	-95.75	7%
Max Normal Stress-Z tubes (MPa)	42.342	65.41	-54%
Max Equivalent Stress Steel Parts (MPa)	410.5	388.58	5%
Volume (m^3)	0.19481	0.19481	0%
Mass (kg)	536.48	1501.4	-180%

CONCLUSION

This paper conducted a detailed finite element analysis of a bamboo girder for an emergency bridge system. The girder was made primarily from bamboo with some steel parts to hold the bamboo tubes together ens, where they work as one unit and provide a way to connect multiple segments as needed. The following points were concluded from this study:

- The four-point flexural experimental tests on individual culms showed that the material failed locally due to crushing and splitting. The average modulus of elasticity was 14583 MPa, and the average ultimate strength was 263 MPa.
- The maximum deflection was 84.68 mm, exceeding the limit of L/100, which is 77.48 mm. It indicates that a fully loaded pickup truck might be too heavy for the serviceability requirements of this girder.

- For the bamboo tubes, the maximum equivalent von-Mises stress reached 85 MPa, much lower than the design strength of 175 MPa. Moreover, the maximum normal compressive stress was 102.5 MPa, and the maximum normal tensile stress was 42.3 MPa along the longitudinal axis Z, lower than the design strength of 175 MPa.
- The steel parts had a stress of 410 MPa at a single node, exceeding the yield strength of 250 MPa but lower than the ultimate strength of 460 MPa. This high stress could be explained by numerical inaccuracy.
- The comparison with an identical girder using steel tubes showed that the steel girder resulted in lower deflection but significantly higher equivalent stresses. However, its weight was 180% higher than that of the bamboo girder, making it more difficult to transport and deploy quickly during emergencies.

ACKNOWLEDGEMENT

The authors thank everyone who has contributed to this project directly or indirectly.

REFERENCES

Akinlabi, E. T., Anane-Fenin, K., & Akwada, D. R. (2017). *Bamboo the multipurpose plant*. Springer International Publishing. https://doi.org/10.1007/978-3-319-56808-9

Amede, E. A., Hailemariama, E. K., Hailemariam, L. M., & Nuramo, D. A. (2021). A review of codes and standards for bamboo structural design. *Advances in Materials Science and Engineering*, *2021*, Article 4788381. https://doi.org/10.1155/2021/4788381

Ansys Inc. (2017). *ANSYS theory reference* (Release 18.2). https://www.ansys.com/

Auwalu, F. K., & Dickson, P. D. (2019). Bamboo as a sustainable material for building construction in Nigeria. *Civil and Environmental Research*, *11*(8), 30–36. https://doi.org/10.7176/CER/11-8-03

Bahari, S. A., & Krause, A. (2016). Utilizing Malaysian bamboo for use in thermoplastic composites. *Journal of Cleaner Production*, *110*, 16–24. https://doi.org/10.1016/j.jclepro.2015.03.052

Chung, K. F., & Yu, W. K. (2002). Mechanical properties of structural bamboo for bamboo scaffoldings. *Engineering Structures*, *24*(4), 429–442. https://doi.org/10.1016/S0141-0296(01)00110-9

Egoh, A., Reed, K. S., & Kalu, P. N. (2020). A review of the current status of bamboo usage with special emphasis on orthopedic rehabilitation. *Materials Sciences and Applications*, *11*(07), 415–430. https://doi.org/10.4236/msa.2020.117028

ISO 22157-2:2004. (2004). *Bamboo-Determination of physical and mechanical properties-Part 2: Laboratory manual*. https://www.iso.org/standard/38360.html

Liu, K. W., Xu, Q. F., Wang, G., Chen, F. M., Leng, Y. B., Yang, J., & Harries, K. A. (2022). Types and characteristics of bamboo materials for construction uses. In K. W. Liu, Q. F. Xu, G. Wang, F. M. Chen, Y. B. Leng, J. Yang & K. A. Harries (Eds.), *Contemporary Bamboo Architecture in China* (pp. 7–30). Springer. https://doi.org/10.1007/978-981-16-8309-1_2

Liu, W., Hui, C., Wang, F., Wang, M., & Liu, G. (2018). Review of the resources and utilization of bamboo in China. In Khalil H. P. S. A. (Ed.), *Bamboo - Current and Future Prospects* (pp. 133-142). IntechOpen. https://doi.org/10.5772/intechopen.76485

Musthaffa, A. A., Nor, N. M., Yusof, M. A., & Yuhazri, M. Y. (2018). New conceptual design of portable bamboo bridge for emergency purposes. *AIP Conference Proceedings*, *1930*(1), Article 20043. https://doi.org/10.1063/1.5022937

Najeeb, M. I., Syamsir, A., Amir, S. M. M., Khan, T., & Sebaey, T. A. (2023). Failure analysis of plant fibre-reinforced composite in civil building materials using non-destructive testing methods: Current and future trend. *Journal of Natural Fibers*, *20*(2), Article 2246654. https://doi.org/10.1080/15440478.2023.2246654

Rahman, M. A., Haque, S., Athikesavan, M. M., & Kamaludeen, M. B. (2023). A review of environmental friendly green composites: Production methods, current progresses, and challenges. *Environmental Science and Pollution Research*, *30*(7), 16905–16929. https://doi.org/10.1007/s11356-022-24879-5

Rong, K., Ekeland, A., Shao, C., Zhang, Y., & Shangguan, S. (2022). Bamboo bridges: A nature-based Solution. *Green Building & Construction Economics, 3*(1), 12–26. https://doi.org/10.37256/gbce.3120221307

Salzer, C., Wallbaum, H., Lopez, L. F., & Kouyoumji, J. L. (2016). Sustainability of Social housing in asia: A holistic multi-perspective development process for bamboo-based construction in the Philippines. *Sustainability, 8*(2), Article 151. https://doi.org/10.3390/su8020151

Technical Committee CEN. (2003). *Eurocode 1: Actions on structures - Part 2: Traffic loads on bridges*. https://knowledge.bsigroup.com/products/eurocode-1-actions-on-structures-traffic-loads-on-bridges

Yan, X., Quan, Z., & Bo, S. (2010). Design and construction of modern bamboo bridges. *Journal of Bridge Engineering*, *15*(5), 533–541. https://doi.org/10.1061/(ASCE)BE.1943-5592.0000089

Yang, D., Li, H., Xiong, Z., Mimendi, L., Lorenzo, R., Corbi, I., Corbi, O., & Hong, C. (2020). Mechanical properties of laminated bamboo under off-axis compression. *Composites Part A: Applied Science and Manufacturing*, *138*, Article 106042. https://doi.org/10.1016/j.compositesa.2020.106042